

# Monitoring of Strains and Deflections of a Steel Cantilever, using a Contactless Measurement Method

Ladislav Galdun<sup>1,2</sup>, Mohamad Al Ali<sup>3\*</sup>, Peter Platko<sup>3</sup>,  
Stanislav Kmet'<sup>3‡</sup>, Vincent Kvočák<sup>3</sup>, Rastislav Varga<sup>1,2</sup>

<sup>1</sup> RVMagnetics a.s., Nemcovej 30, 04001, Košice, Slovakia  
galdun@rvmagnetics.com, varga@rvmagnetics.com

<sup>2</sup> Center for Progressive Materials, Technology and Innovation Park, Pavol Jozef Šafárik University in Košice, Tr. SNP 1, 04011 Košice, Slovakia

<sup>3</sup> Institute of Structural and Transportation Engineering, Faculty of Civil Engineering, Technical University of Košice, Vysokoškolská 4, 04200, Košice, Slovakia  
mohamad.alali@tuke.sk\*, peter.platko@tuke.sk, stanislav.kmet@tuke.sk

---

*Abstract: The aim of the experimental and analytical work was to monitor and analyze the strains and deflections of steel cantilevers using a bistable glass-coated microwire, as a contactless measurement method. For verification and comparison, the results obtained from the applied bistable microwire ( $Fe_{75}Si_9B_{10}P_5Tb_1$ ), the results of a standard resistance strain gauge and dial indicator were used. Since the microwire used, has a metallic (magnetic) core, verifying the possibility of separating the influence of the parasitic external magnetic field from the measured deformations, was the first goal of the implementation of the bending test on steel cantilevers. Another goal was to find a relationship between the switching field of the microwire and the strains measured by the strain gauge, depending on the applied load during the experimental test. Both goals were achieved within this research.*

*Keywords: Contactless; Bistable microwire; Magnetic field; Strain; Strain gauge*

---

## 1 Introduction

Experimental tests with the application of resistance strain gauges, dial indicators and similar conventional sensors are used for monitoring and recording the stress state and strain development in tested structural members, as well as to support the results of theoretical and numerical analyzes of such members [1-5]. During experimental tests and loading processes, conventional sensors must be

permanently connected to computers and evaluation devices using various types of data acquisition systems - data buses [6-9]. This fact limits the possibility of using strain gauges and dial indicators only for laboratory conditions. The need to protect sensing technologies from weather effects have limited their outdoor use for monitoring existing structural members and structures. In addition, the necessity of permanently connecting the recording devices until the end of the measurement process makes it impossible to use these devices simultaneously in another experimental investigation.

Since contactless methods allow monitoring and recording the stress state of the investigated members without the need for their permanent connection to recording devices, these methods are becoming more convenient and flexible for structural engineers and researchers. One of the possibilities of contactless measurement is the use of bistable glass-coated microwires [10-12]. Due to their magnetic properties, it is possible to perform contactless measurements of strains by means of an induction method via a sensing unit. The microwire, as a passive part of the system, can be placed at any location; moreover, it can even be embedded inside the material of the tested member [13-15].

The mentioned disadvantages of standard strain gauges can be avoided by using a bistable microwire, as the presented research shows. On the other hand, the analyzes presented in this work represent a new concept of contactless strain measurement applied to a steel (ferromagnetic) structural member. As stated in the paper, this method allows for separation of the influence of parasitic magnetic fields that can occur when measuring magnetic materials.

## 2 Applied Microwire and Method of Analysis

In the performed experiment, a glass-coated microwire  $\text{Fe}_{75}\text{Si}_9\text{B}_{10}\text{P}_5\text{Tb}_1$  with a metal core of  $10\ \mu\text{m}$  in diameter and a total diameter of  $30\ \mu\text{m}$  was used. Figure 1 shows a typical micrograph of a microwire with a partially removed glass coating.

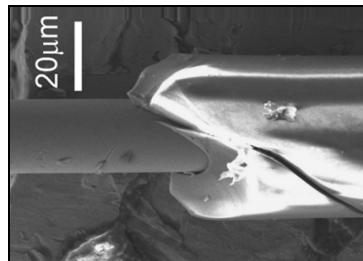


Figure 1

Micrographic configuration of a glass-coated microwire

## 2.1 Microwire Response Measurement

The magnetic response of the bistable glass-coated microwire is given by the switching field  $H_{SW}$ . The induction method was used to measure this magnetic response. A typical square magnetic hysteresis loop and switching field  $H_{SW}$  is illustrated in Figure 2, where  $M_S$  is the saturation magnetization and  $H$  is the magnetic field.

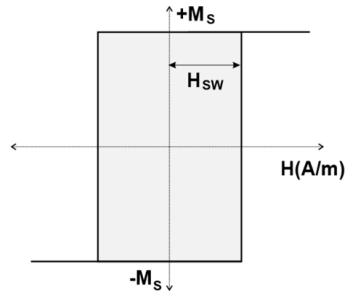


Figure 2

Magnetic hysteresis loop with switching field  $H_{SW}$

Monitoring the response of the microwire was realized using a sensing system placed above the microwire. The 70x20x20 mm sensing system has two tapes to create a gap of about 2 mm between the sensing system and the microwire, as shown in Figure 3. The height of the tape depends on the required height of the gap and the type of microwire used. So, the distance between the sensing system and the microwire can be increased to about 50 mm.

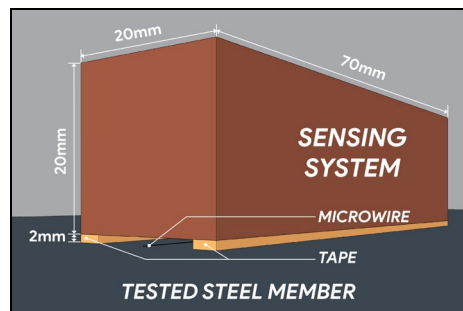


Figure 3

Illustration of the sensing system

A pair of coils is integrated in the sensing system. The first of these is the excitation coil. This coil generates a magnetic field for the magnetization reversal process of the microwire. To achieve the magnetization reversal process, the excitation coil was powered by a triangular AC voltage with a frequency of 100 Hz and 7.44 V amplitude. The second one is the pickup coil, in which the

magnetization reversal process of the microwire is detected and transformed into the sensing signal. Figure 4 presents the above-mentioned magnetization reversal process. The yellow lines represent the excitation signal, while the sensing signal with two maximum and minimum peaks is blue.  $t_1$  and  $t_2$  are the time occurrence of positive and negative switching between two states of magnetization  $\pm M_S$  (the time of the magnetization reversal of the microwire).

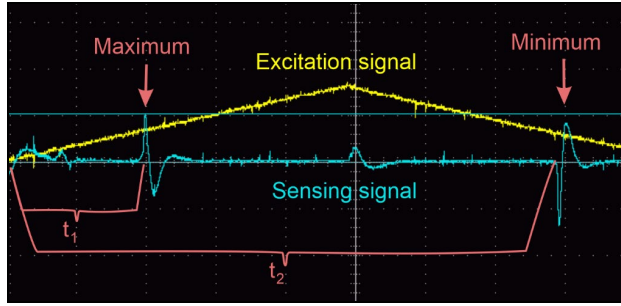


Figure 4

Graphical visualization of the excitation and sensing signal

## 2.2 Application of the Induction Method

As mentioned in the previous chapter, a triangular AC voltage was used to create the magnetic field. The obtained switching field  $H_{SW}$  is commensurable to the stress caused by the applied load, under conditions of constant temperature and excitation field frequency [11]:

$$H_{SW} = \frac{\sqrt{A \cdot \lambda_S \cdot \sigma}}{\mu_0 \cdot M_S} \quad (1)$$

where:  $A$  is the exchange constant  
 $\lambda_S$  is the saturation magnetostriction  
 $\sigma$  is the stress caused by the applied load  
 $\mu_0$  is the vacuum permeability  
 $M_S$  is the saturation magnetization

Because of the positive magnetostriction of the metallic core, the microwire is sensitive to the strain  $\varepsilon$ , transmitted from the applied load and corresponding stress. The strain follows Hooke's law. It follows that the switching field is proportional to the relative elongation of the tested member, to which the microwire is fixed (glued). The switching field  $H_{SW}$  is also proportional to the switching time  $t_{SW}$  (see Figure 4), which is the magnetization reversal time of the microwire:

$$t_{sw} = t_1 + t_2 \quad (2)$$

Equation 2 is also applicable in the case when an additional parasitic external magnetic field is present. The external magnetic field does not influence the width of the hysteresis loop ( $H_{sw}$ ) and, thus, the  $t'_{sw}$  (Equation 3). On the other hand, the position of the hysteresis loop is shifted depending on the direction of the magnetic field, Figure 5 [12]. In other words, when an external magnetic field is present, the center of the hysteresis loop (Figure 2) shifts, as shown in Figure 5.

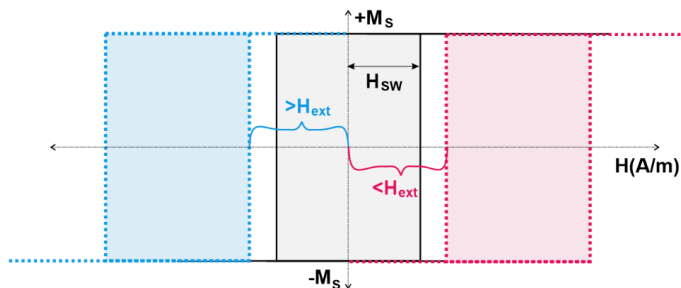


Figure 5

The shift of the hysteresis loop caused by parasitic external magnetic field

This phenomenon provides the possibility of identifying the direction and amplitude of the external magnetic field. The difference in the switching time  $t'_{sw}$ , which is proportional to the external magnetic field, can be achieved using Equation 3 [12]:

$$H_{ext} \approx t'_{sw} = t_2 - t_1 \quad (3)$$

According to the presented approach, it can be concluded that it is possible to separate the magnetic influence of the environment (parasitic external magnetic field) from the required measurements, which is very necessary when testing magnetic (steel) material.

### 3 Preparation for the Experimental Test

#### 3.1 Production of Experimental Test Components

Three specimens made from sheet material of low-carbon steel S 235 were fabricated to perform the bending test of the cantilever. The specimens have a cross-section of 80x3 mm and a length of 600 mm. A hole was drilled on one side of the specimens to fix the pre-prepared loading mechanism. Figure 6 shows the steel specimen prepared for the test, including the place of the cantilever fixing,

the position of sensing devices and the location of the loading mechanism connection (hole).



Figure 6

Steel specimen prepared for bending test

A special loading mechanism was designed and produced for experimental tests, as shown in Figure 7. This mechanism, made of galvanized steel, consists of two parts:

- Load carrier, designed to ensure the vertical action of the force during the cantilever deflection process, thanks to the hinge connection that allows the system to rotate. The load carrier weighs about 787 g
- Weights with dimensions 80x84x5 mm, having holes in the middle. The length of approximately 84 mm has been adjusted so that each weight had a mass of 250 g ( $\pm 2$  g). The holes allow for easy increase and/or decrease of load size.



Figure 7

Loading mechanism - load carrier and loading weights

### 3.2 Preparation of Supporting Materials

The preparatory works included numerical analysis to estimate the theoretical elastic resistance moment of the steel cantilever, strains and deflections. A schematic representation of the cantilever with the measurement locations of strains ( $x_s$ ), deflections ( $x_f$ ) and the position of the applied force ( $x_f$ ) is in Figure 8.

The used steel has nominal values of material properties:  $f_y = 235$  MPa (Yield stress),  $f_u = 360$  MPa (Ultimate stress) and Young's modulus  $E = 210\,000$  MPa [16] [17].

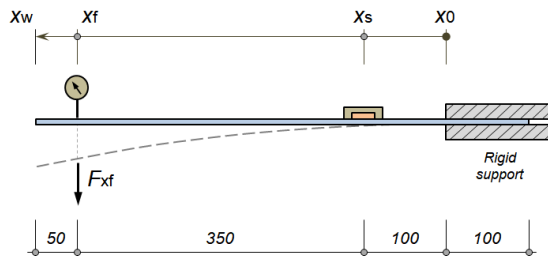


Figure 8

Schematic representation of the cantilever

According to the above-mentioned material properties and Figure 8, the cross-sectional elastic resistance moment was determined at the fixed point ( $x_0$ ) and had the value:  $M_{el,Rd} = 28.20$  Nm. This moment was achieved from the applied force  $F_{xf,max} = 57.43$  N. At this load level, the deflection in the position ( $x_w$ ) had a value of 57.74 mm.

To ensure the elastic behavior of the cantilever, the maximum load for the experimental test was set to about 70% of the theoretically determined maximum load  $F_{xf,max}$ , i.e.,  $F_{xf,70} = 40.20$  N. According to  $F_{xf,70}$ , a sequence of load steps was created and divided into 15 load cases (LC) as shown in table 1. Table 1 also contains the calculated values of the applied force, corresponding stress and strain for each load case.

Table 1

Load cases with relevant forces, stresses and strains

Load case	Acting force $F_{xf}$ [N]	Normal stress $\sigma_{x_0}$ [kPa]	Strain $\epsilon_{ss}$ [%]
LC1 = $G$	-	19625	0.006
LC2 = $G + F_0$	7.87	49138	0.017
LC3 = $G + F_0 + F_1$	10.37	58513	0.020
LC4 = $G + F_0 + F_2$	12.87	67888	0.024
LC5 = $G + F_0 + F_3$	15.37	77263	0.027
LC6 = $G + F_0 + F_4$	17.87	86638	0.031
LC7 = $G + F_0 + F_5$	20.37	96013	0.034
LC8 = $G + F_0 + F_6$	22.87	105388	0.038
LC9 = $G + F_0 + F_7$	25.37	114763	0.041
LC10 = $G + F_0 + F_8$	27.87	124138	0.045
LC11 = $G + F_0 + F_9$	30.37	133513	0.048
LC12 = $G + F_0 + F_{10}$	32.87	142888	0.052

$LC13 = G + F_0 + F_{11}$	35.37	152263	0.055
$LC14 = G + F_0 + F_{12}$	37.87	161638	0.059
$LC15 = G + F_0 + F_{13}$	40.37	171013	0.062

Where:  $G$  is the dead load of the cantilever,  $F_0$  is the weight of the load carrier,  $F_i$  is the applied force achieved by gradually adding weights in the respective load case ( $i = 1$  to 13).

## 4 Implementation of the Bending Test

In the beginning, bistable glass-coated microwire  $Fe_{75}Si_9B_{10}P_5Tb_1$  was fixed on the surface of the steel specimen using glue X60 based on methyl-methacrylate. Strain gauge FLAB-6-11 was glued, using the same type of glue, close to the microwire to obtain comparable results. Moreover, a dial indicator (DI) was added to the measurement system, near the free end of the cantilever, to monitor the deflections. The layout of the test and the locations of the measuring devices are illustrated in Figure 9.

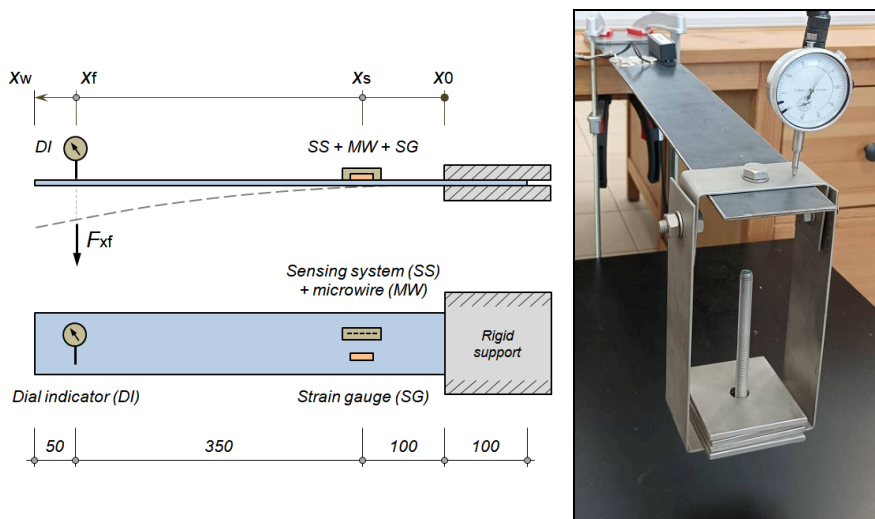


Figure 9

General view of the test arrangement

The switching time was obtained by placing the sensing system (SS), connected to an oscilloscope, over the microwire (MW) to monitor its response (Figure 3). Then the sensing signal was displayed on the oscilloscope (Figure 4) in the shape of minimum and maximum peaks. After that, the position of the peaks was determined manually, taking into account the time range of the oscilloscope.

The strains were measured by connecting the strain gauge to a computer via calibrated data-bus MX1615B. A quarter-bridge was used to connect the strain gauge (SG) to the data-bus. Catman Easy V5.1.3 software was used for data recording and evaluation.

The strain, deflection and switching time measuring devices were set to zero before the load carrier was installed, and this state was considered the first load case. As a second load case, after installing the load carrier, a weight of 787 g was set, and the changes in strain, deflection and microwire switching time values were recorded. Then the load was gradually increased up to 4037 g by sequentially adding 13 weights, see table 1, while simultaneously recording the changes in strain, deflection and switching time of the microwire step by step. After reaching a weight of 4037 g, the test continued with the unloading process by sequentially removing the 13 weights, so the load returned to a weight of 787 g (load case no. 2).

The load was applied only within the elastic zone of the used steel, i.e., the plasticization and hardening zones with plastic strains were not reached.

## 5 Results and Discussion

The measured output data from the experimental test during the loading and unloading process are presented in Figures 10, 11 and 12. The relationship between the applied forces and deflections, in relation to individual load cases, is given by Figure 10. Figure 11 illustrates the development of the strains, and Figure 12 shows the variation of the microwire switching time.

As shown in the graphs, the strains (measured by strain gauge) and deflections (measured by dial indicator) have a linear shape, which ensures that the measurement was carried out within the elastic zone of the material used (S 235). The switching time of the microwire obtained by the contactless measurement method has a quasi-linear character in a similar shape, compared to the deflections and strains. At the maximum load of 40.37 N (load case no. 15), the deflection reached a value of 41.7 mm at a measured strain value of 0.065% and the maximum change of the switching time was 0.4 ms.

Using the results to determine the relationship between the strains and the switching times, the correlation for linear fit was determined as  $y=0.14x-1.38$  (Fig. 13). The black spots are experimental results and the orange line is the correlation between switching time (X-axis) and strains (Y-axis).

As part of their previous experimental research, the authors already proved the possibility of using the above-mentioned contactless method for measuring the strains of a non-magnetic material via a bistable microwire [18]. The possibility of

using this method for magnetic material was experimentally investigated and presented in this paper.

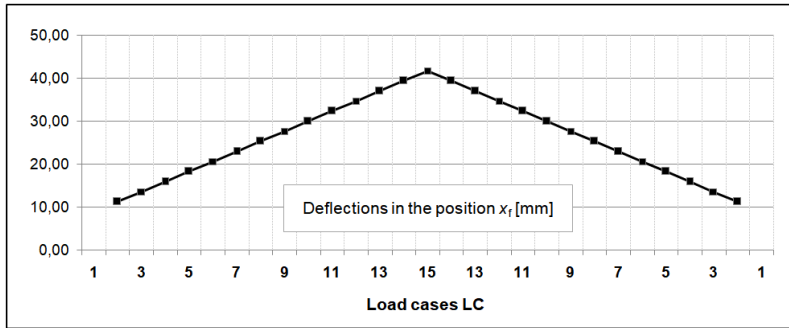


Figure 10  
Relationship between the applied forces and deflections

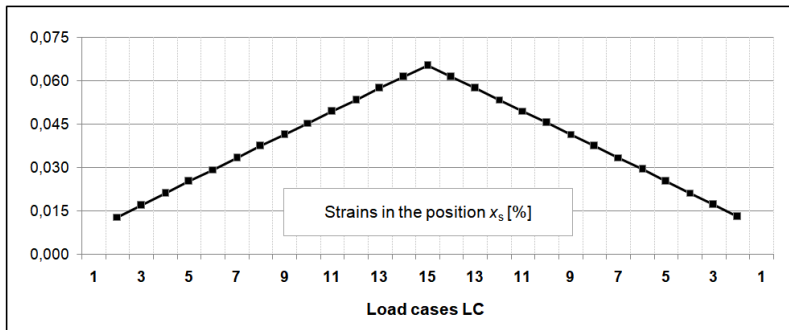


Figure 11  
Relationship between the applied forces and strains

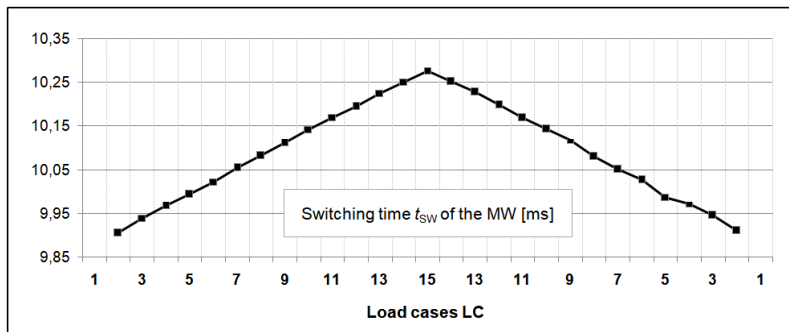


Figure 12  
Relationship between the applied forces and switching time

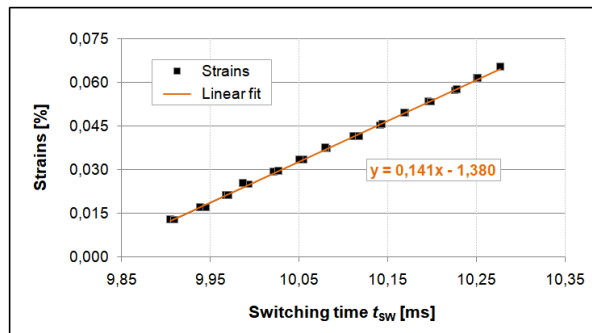


Figure 13

Dependence of switching time on strains

## Conclusions

As presented and proven in this paper, thanks to the magnetic bistability of the microwire, it was possible to perform a contactless measurement, on a metal member with magnetic properties.

The obtained results also demonstrated a comparable character in the behavior of the applied sensing devices (strain gauge, dial indicator and microwire) during the loading and unloading process. Furthermore, due to the linear nature of the results, the relationship between strains and switching time for this relevant case was determined, as shown in Figure 13.

Taking into account the above-mentioned results, glass-coated bistable microwires can be considered as suitable candidates for contactless measurement of elastic strains, when investigating materials of ferromagnetic character.

After achieving adequate results in the elastic zone of the used material, future research work will be focused on the application of glass-coated bistable microwires, to measure strains within the elasto-plastic and hardening zones of the various materials that make up structural members.

## Acknowledgement

This work was supported by the Slovak projects APVV-15-0777, APVV-16-0079, Slovak VEGA grants no. 1/0129/20 and 1/0172/20.

## References

- [1] Wang B., Ke X., Du K., Bi X., Hao P., Zhou C., A novel strain field reconstruction method for test monitoring, *International Journal of Mechanical Sciences*, 243 (2023)
- [2] Zhou C., Xia M., Xu Z., Design and optimization of a quadrupedal dynamic disturbance force measurement platform using strain gauges, *Mechanical Systems and Signal Processing*, 188 (2023)

- 
- [3] Mokhtari E., Palermo M., Laghi V., Incerti A., Mazzotti C., Silvestri S., Quasi-static cyclic tests on a half-scaled two-storey steel frame equipped with Crescent Shaped Braces at both storeys: Experimental vs. numerical response, *Journal of Building Engineering*, 62 (2022)
- [4] Hu X., Li Y., Zhang H., Yu Y., Kang Z., Design and Application of Automatic Calibration Device for Multi-Channel Resistance Strain Gauge Indicator, *Journal of Physics: Conference Series*, 2113/1 (2021)
- [5] Daou A., Chehab G., Saad G., Hamad B., Experimental and numerical investigations of reinforced concrete columns confined internally with biaxial geogrids, *Construction and Building Materials*, 263 (2020)
- [6] Meyland M. J., Eriksen R. N. W., Nielsen J. H., A modified split-Hopkinson pressure bar setup enabling stereo digital image correlation measurements for flexural testing, *International Journal of Impact Engineering*, 173 (2023)
- [7] Gioiosa A., Bonventre R., Donati S., Flumerfelt E., Horton-Smith G., Morescalchi L., O'Dell V., Pedreschi E., Pezzullo G., Spinella F., Uplegger L., Rivera R. A., Slow control and data acquisition systems in the Mu2e experiment, *Proceedings of Science*, 380 (2022)
- [8] Yang T., Wang W., Huang Y., Jiang X., Zhao X., Accurate Monitoring of Small Strain for Timbre Recognition via Ductile Fragmentation of Functionalized Graphene Multilayers, *ACS Applied Materials and Interfaces*, 12/51 (2020)
- [9] Doggett W., Vazquez S., Architecture for real-time interpretation and visualization of structural sensor data in a laboratory environment, *AIAA/IEEE Digital Avionics Systems Conference - Proceedings*, 2 (2000), pp. 6.D.2-1-6.D.2-8
- [10] Praslicka D., Blazek J., Smelko M., Hudák J., Cverha A., Mikita I., Varga R., Zhukov R. A., Possibilities of measuring stress and health monitoring in materials using contact-less sensor based on magnetic microwires, *IEEE Trans. Magn.* 49 (2013) 128-131
- [11] Varga R., Gamcova J., Klein P., Kovac J., Zhukov A., Tailoring the switching field dependence on external parameters in magnetic microwires, *IEEE Trans. Magn.* 49 (2013) 30
- [12] Jacko P., Jurč R., Galdun L., Hvizdoš L., Kováč D., Varga R., Linear position sensor using magnetically bistable microwire. *Sens. Actuators A Phys.* (2023), 349, 114017
- [13] Kohan M., Varga R., Hudak R., Schnitzer M., Ferencik N., Dancakova G., Lancos S., Anonymous Pilot study: Measurement of mechanical load using a glass-coated microwire for implantology applications. *SAMI 2021 - IEEE 19<sup>th</sup> World Symposium on Applied Machine Intelligence and Informatics, Proceedings* (2021), 267-272

- 
- [14] Olivera J., Aparicio S., Hernández M. G., Zhukov A., Varga R., Campusano M., Echavarria E., Velayos J. J. A., Microwire-based sensor array for measuring wheel loads of vehicles. *Sensors* 2019, 19, (21), 4658
- [15] Sabol R., Klein P., Ryba T., Hvizdos L., Varga R., Rovnak M., Sulla I., Mudronova D., Galik J., Polacek I., Zivcak J, Hudak R., Novel Applications of Bistable Magnetic Microwires. *Acta Phys. Pol.* 131 (4): 1150-1152
- [16] STN EN 1993-1-1 Eurocode 3: Design of steel structures, Part 1-1: General rules and rules for buildings, SÚTN, 2006
- [17] STN EN 10025-2:2019. Hot rolled products of structural steels. Part 2: Technical delivery conditions for non-alloy structural steels
- [18] Al Ali M., Platko P., Bajzecerova V., Kmet S., Galdun L., Spegarova A., Varga R., Monitoring the strain of beech plywood using a bistable magnetic microwire, *Sens. Actuators A: Phys.* 326 (2021) 112726